American Mineralogist, Volume 61, pages 1213–1225, 1976

The crystal structures of high albite and monalbite at high temperatures

C. T. PREWITT, S. SUENO[1] AND J. J. PAPIKE

Department of Earth and Space Sciences
State University of New York
Stony Brook, New York 11794

Abstract

X-ray diffraction data obtained at 24, 300, 600, 750, 900, 1090, and 1105°C have been used to investigate the crystal structure of high albite at high temperatures. These results show that, for the models tested, splitting of Na into four quarter-atoms gives the best agreement between the structure model and X-ray intensities. At high temperatures, albite twinning and broadened diffraction peaks make detection of the albite–monalbite transition difficult; however, these single crystals of synthetic high albite ($Or_{0.5}Ab_{98.3}An_{1.2}$) were not monoclinic at 1105°C. This contrasts with other investigations where the high albite–monalbite transition has been reported to occur at temperatures as low as 930°C. Possible reasons for these discrepancies include different prior thermal histories, the presence of polysynthetic twinning and/or other defects in crystals transforming at the lower temperatures, different compositions for the crystals, and errors in measurement of the transition point. Although no direct evidence has been found for a domain structure in high albite, a possible explanation for the observations is that four kinds of domains or regions exist in the crystal, each of which contains an ordered triclinic arrangement of $AlSi_3$, but with Al occupying a different one of the four possible tetrahedral sites in the crystal structure comprising each region. Each Na position is then a function of the immediate Al/Si environment.

Introduction

Ferguson *et al.* (1958) reported the first refinements of the structures of low albite and high albite. In that paper several questions were raised about the structures which have not yet been answered satisfactorily. These questions involve the nature of the Na atom and the degree of Al/Si disorder in the low- and high-albite structures. These authors found that the Na atom in low albite has an unusually anisotropic thermal vibration which could be interpreted as thermal vibration or as a random occupancy of one of two positions separated by ~ 0.1Å in the relatively large cavity in which Na resides. The anisotropic character of Na in high albite was found to be even greater, with a separation for the split atom model of approximately 0.6Å. The problem was reviewed again by Ribbe *et al.* (1969) using new three-dimensional X-ray data. In their paper the problem and experimental evidence were more clearly defined; however, the conclusion for low albite was that neither of the possible models could be ruled out by the evidence at hand. For high albite the evidence was again not definitive, but the best match to the data was obtained using a quarter-atom model with four quarter-atoms distributed in an approximate line along the major axis of the anisotropic Na Fourier peak and with separations of 0.9Å between the outer pair and 0.2Å between the inner pair. Although there is some discussion of possible domain structures in high albite in Ribbe *et al.* (1969), and although Quareni and Taylor (1971) reported on a high-temperature study of low albite, the behavior of the Na atom in albite is still not well understood.

With regard to the question of Al/Si ordering in albite, one would like to know whether low albite is completely ordered and high albite completely disordered; also, there is the question of whether intermediate albites exist, and if so, whether the lattice parameters change in a regular way as a function of Al/Si ordering. Ribbe *et al.* (1969) concluded that Al is ordered into one site and Si into the other three

[1] Present address: Institute of Geoscience, University of Tsukuba, Ibaraki, 300-31, Japan

sites in low albite, even though the three Si sites differ slightly in average T–O distance. They also concluded that Al is distributed randomly over the four sites in high albite even though the tetrahedron equivalent to the Al tetrahedron ($T1o$) is slightly larger than the other three in high albite. In a much more detailed analysis, Phillips and Ribbe (1973) confirmed these conclusions. Other work, such as that of Harlow *et al.* (1973), has not significantly changed this interpretation of Al/Si order in low albite and high albite.

Another aspect of albite structural chemistry which has been the subject of discussion is whether there is a transition from triclinic to monoclinic symmetry in high albite at high temperature (~ 1000°C). The literature on this subject is extensive and has been reviewed in detail by Smith (1974). Questions revolve around the source and prior heat treatment of the albite, the type of experiment used to determine the temperature of transition, and the nature of monalbite itself.

Because all of the points raised above were of interest to us, we decided to undertake a structural study of albite single crystals at high temperature in order to solve the problems outlined above or to add additional information which would provide better understanding of the problems and their solutions. This paper reports results obtained from our investigation of high albite crystals synthesized hydrothermally and annealed at 1060°C for 40 days. Preliminary results were reported by Sueno *et al.* (1973) and Prewitt *et al.* (1974). Subsequent to these reports, Okamura and Ghose (1975) investigated the transition to monalbite using annealed Amelia albite crystals. Because the results of the two investigations differ in important ways, the differences are discussed here in detail.

Experimental

Nomenclature

Different authors have used different symbols for labelling the atom sites in albite. Most of these are based on a paper by Megaw (1956) which was, in turn, based on the original notation of Taylor (1933). We follow the scheme used by Megaw (1974), but without parentheses or subscripts to aid typing and typesetting. For example, Megaw (1974) labelled the tetrahedral sites $T_1(o)$ and $T_1(m)$ where o and m stand for *original* and *mirror*. We use $T1o$ and $T1m$ with similar modification for the other sites.

Another use of nomenclature concerns the terms high albite and analbite. Laves (1960) defined analbite as a triclinic albite which will invert to monalbite at high temperature and high albite as a triclinic albite that will not invert to monalbite. Because there is probably a continuous series between lowest and highest albite structural states and because there is some uncertainty about the existence of truly monoclinic albite, we will use the terms suggested by Smith (1974, p. 446), *i.e., maximum low albite* and *maximum high albite* to describe albites which are at the extremes of order and disorder. For structural states near the extremes, where exact designation of structural state is not important, the prefix *maximum* will be dropped. When the structural state is clearly between the extremes, *intermediate albite* will be used.

Source of crystals

Intermediate albite crystals synthesized at 700°C and 5 kbar under hydrothermal conditions were obtained from Dr. G. Lofgren (Johnson Space Center, Houston, Texas). These crystals were annealed at 1060°C for 40 days in an evacuated silica-glass tube. The chemical composition of these crystals is discussed in a later section of this paper. Twin-free single crystals approximately 100 μm in diameter were carefully selected using precession camera X-ray photography. For high-temperature experiments, these crystals were mounted parallel to a^* on silica-glass fibers with mullite "glass" cement and then sealed in evacuated silica-glass capillaries. The details of the crystal heater and the high-temperature cement were discussed by Brown *et al.* (1973).

Intensity and cell parameter measurement

Integrated intensities were measured at several temperatures (24, 300, 600, 750, 900, 1090, and 1105°C) using a computer-controlled Picker four-circle diffractometer with Mo$K\alpha$ radiation (0.7107Å) monochromatized with a graphite crystal. The reflection data were measured using an ω–2θ scan (2°/minute) with ten-second background counts on either side of the peak and were converted to structure factors by applying Lorentz and polarization corrections, but no absorption corrections. To maintain uniformity in the intensity measurement, we attempted to collect the same set of reflections within a 2θ range 5°–60° at each temperature. A standard reflection, 060, was monitored once for every 20 reflections throughout each data collection. After each set of intensity data was obtained, cell-parameter determinations at the appropriate temperature were made using over 35 independent 2θ values and the CELRF least-squares program written by Prewitt. Fi-

nal cell parameters associated with each set of intensity data plus several for other temperatures are listed in Table 1.

Refinement

All refinements of structure models were run using space group $C\bar{1}$, neutral atom scattering factors (Doyle and Turner, 1968), and the full-matrix, least-squares refinement program, RFINE, written by L. W. Finger (Geophysical Laboratory). All intensities were weighted according to $w = 1/\sigma_F$ where σ_F is the standard error based on counting statistics (Prewitt and Sleight, 1968). All reflections which were indistinguishable from background or which had asymmetric backgrounds were rejected from the refinements. High albite was refined using two different models, with sodium included as a single atom or four quarter-atoms. Also, high-albite data collected at 1090°C were used to test a model where all atoms were split into four positions, but this model did not converge. The numbers of collected reflections (excluding the standard reflection 060), the numbers of reflections which were used for the final cycle of refinement, and the final R factors are given in Table 2. Table 3,[2] which contains the structure factors and the parameters from the last cycle of each refinement series, has been deposited with the Mineralogical Society of America.

The results of the refinements of high-albite structures at different temperatures are reported as follows: positional parameters and isotropic temperature factors (Table 4); T–O distances, O–O distances in the tetrahedra, and Na–O interatomic distances (Table 5).

TABLE 2. Intensity data for high albite

Temp. (°C)	No. Refl.	R_1	R_1'	$R_{1/4}$	$R_{1/4}'$
24	1843	4.8(1731)*	4.6(1731)*	4.1(1730)*	3.7(1730)*
350	1856	5.2(1734)	4.8(1734)	4.9(1734)	4.4(1734)
600	1873	5.4(1739)	5.1(1739)	5.2(1741)	4.8(1741)
750	1877	5.5(1720)	5.2(1720)	5.3(1720)	5.0(1720)
950	1893	5.3(1712)	5.2(1712)	5.2(1712)	5.1(1712)
1090	1907	7.7(1686)	7.3(1686)	7.7(1686)	7.3(1686)
1105	1753	6.8(1577)	6.5(1577)	6.8(1576)	6.5(1576)

$R = \Sigma||F_o| - |F_c||/\Sigma|F_o|$, $R' = \Sigma w(|F_o| - |F_c|)^2/\Sigma w(|F_o|)^2$.

R_1 *is for a single anisotropic Na atom.*

$R_{1/4}$ *is for four isotropic quarter Na atoms.*

* *Numbers in parentheses represent the number of reflections used in final refinement.*

Triclinic–monoclinic transition

As stated previously, the crystals were heated at 1060°C for forty days with the intention of producing maximum high albite. However, in the high-temperature experiments, our crystals were not monoclinic at 1105°C. We did not examine high albite at above 1120°C, because the softening of the silica-glass fiber on which the crystal was mounted causes slight movement of the crystal and results in a decrease in the accuracy of the unit-cell measurement.

To check our cell-parameter measuring technique, we examined monoclinic K–feldspar at high temperature assuming it to have triclinic symmetry. However, in least-squares refinements, the cells always refined to monoclinic symmetry. The change in cell

[2] To obtain Table 3, order document AM-75-032 from the Business Office, Mineralogical Society of America, LL 1000, 1909 K Street, N.W., Washington, D.C. 20006. Please remit $1.00 in advance for the microfiche.

TABLE 1. Cell parameters of high albite as functions of temperature†

T	a/a^*	b/b^*	c/c^*	α/α^*	β/β^*	γ/γ^*	V/V^*	$\Delta 2\theta$†
24°C	8.1535(4)	12.8694(5)	7.1070(4)	93.521(4)	116.458(3)	90.257(3)	665.95(8)	
	0.137083	0.077900	0.157564	85.938	63.470	87.957	0.001502	2.005
350°C	8.1829(7)	12.8947(6)	7.1190(5)	93.041(5)	116.352(4)	90.172(4)	671.9(1)	
	0.136438	0.077695	0.157048	86.521	63.598	88.300	0.001488	1.698
600°C	8.2096(7)	12.9182(7)	7.1284(4)	92.482(5)	116.282(4)	90.128(5)	677.01(9)	
	0.135891	0.077505	0.156649	87.168	63.685	88.630	0.001477	1.374
750°C	8.2296(7)	12.9336(8)	7.1357(5)	91.956(5)	116.232(4)	90.078(5)	680.8(1)	
	0.135487	0.077376	0.156348	87.781	63.749	88.949	0.001469	1.068
950°C	8.2508(9)	12.9489(9)	7.1431(4)	91.161(5)	116.169(5)	90.030(5)	684.8(1)	
	0.135050	0.077247	0.156025	88.692	63.824	89.396	0.001460	0.624
1090°C	8.2763(10)	12.9593(9)	7.1463(7)	90.097(7)	116.092(6)	89.988(6)	688.4(1)	
	0.134538	0.077165	0.155812	89.898	63.908	89.966	0.001453	0.045
1105°C	8.2783(7)	12.9592(7)	7.1452(5)	90.056(5)	116.087(4)	89.997(4)	688.4(1)	
	0.134500	0.077165	0.155829	89.939	63.913	89.976	0.001453	0.028

† $\Delta 2\theta = 2\theta(131) - 2\theta(1\bar{3}1)$.

Standard errors for direct cell parameters are given in parentheses.

TABLE 4. Atom coordinates and equivalent isotropic temperature factors for high albite

		24°C	350°C	600°C	750°C	950°C	1090°C	1105°C
Na*	x	0.2737 (3)	0.2748 (4)	0.2761 (4)	0.2769 (5)	0.2780 (5)	0.2793 (7)	0.2797 (7)
	y	0.0073 (3)	0.0059 (3)	0.0037 (4)	0.0029 (4)	0.0019 (4)	-0.0000 (6)	0.0000 (6)
	z	0.1329 (5)	0.1348 (6)	0.1374 (7)	0.1374 (7)	0.1371 (7)	0.1377 (11)	0.1382 (10)
	B	7.62 (11)	8.60 (13)	10.02 (14)	10.80 (15)	11.66 (15)	12.67 (22)	12.59 (20)
T1o	x	0.0090 (1)	0.0089 (1)	0.0088 (1)	0.0087 (1)	0.0086 (1)	0.0084 (2)	0.0081 (2)
	y	0.1650 (1)	0.1674 (1)	0.1697 (1)	0.1718 (1)	0.1746 (1)	0.1782 (1)	0.1783 (1)
	z	0.2148 (1)	0.2164 (1)	0.2174 (2)	0.2189 (2)	0.2210 (2)	0.2227 (2)	0.2230 (2)
	B	0.78 (1)	1.22 (2)	1.62 (2)	1.89 (2)	2.17 (2)	2.52 (3)	2.50 (3)
T1m	x	0.0048 (1)	0.0054 (1)	0.0061 (1)	0.0066 (1)	0.0072 (1)	0.0080 (2)	0.0080 (2)
	y	0.8145 (1)	0.8155 (1)	0.8165 (1)	0.8177 (1)	0.8194 (1)	0.8215 (1)	0.8214 (1)
	z	0.2290 (1)	0.2284 (1)	0.2275 (2)	0.2268 (2)	0.2253 (2)	0.2232 (2)	0.2233 (2)
	B	0.78 (1)	1.21 (2)	1.60 (2)	1.85 (2)	2.16 (2)	2.51 (3)	2.53 (3)
T2o	x	0.6902 (1)	0.6919 (1)	0.6931 (1)	0.6940 (1)	0.6951 (1)	0.6962 (2)	0.6963 (2)
	y	0.1079 (1)	0.1096 (1)	0.1110 (1)	0.1123 (1)	0.1141 (1)	0.1160 (1)	0.1160 (1)
	z	0.3202 (1)	0.3242 (2)	0.3281 (2)	0.3316 (2)	0.3363 (2)	0.3418 (3)	0.3420 (2)
	B	0.82 (1)	1.24 (2)	1.62 (2)	1.88 (2)	2.20 (2)	2.53 (3)	2.51 (3)
T2m	x	0.6849 (1)	0.6877 (1)	0.6902 (1)	0.6919 (1)	0.6938 (1)	0.6961 (2)	0.6964 (2)
	y	0.8776 (1)	0.8785 (1)	0.8796 (1)	0.8805 (1)	0.8820 (1)	0.8838 (1)	0.8838 (1)
	z	0.3535 (1)	0.3525 (2)	0.3510 (2)	0.3494 (2)	0.3465 (2)	0.3428 (3)	0.3426 (2)
	B	0.79 (1)	1.23 (2)	1.63 (2)	1.89 (2)	2.21 (2)	2.49 (3)	2.50 (3)
OA1	x	0.0055 (4)	0.0046 (4)	0.0039 (5)	0.0030 (5)	0.0016 (5)	-0.0005 (8)	0.0002 (7)
	y	0.1351 (2)	0.1359 (2)	0.1371 (3)	0.1374 (3)	0.1380 (3)	0.1389 (4)	0.1390 (4)
	z	0.9845 (4)	0.9874 (5)	0.9896 (5)	0.9912 (5)	0.9952 (5)	0.9987 (7)	0.9995 (7)
	B	1.62 (4)	2.44 (5)	3.04 (6)	3.60 (7)	3.98 (7)	4.39 (10)	4.42 (10)
OA2	x	0.5916 (3)	0.5951 (4)	0.5982 (4)	0.6012 (4)	0.6033 (4)	0.6055 (6)	0.6072 (5)
	y	0.9907 (2)	0.9924 (2)	0.9938 (2)	0.9951 (2)	0.9971 (2)	0.9998 (3)	0.9999 (3)
	z	0.2783 (4)	0.2798 (4)	0.2810 (5)	0.2825 (5)	0.2831 (5)	0.2847 (7)	0.2850 (7)
	B	1.32 (4)	1.84 (4)	2.41 (5)	2.85 (5)	3.22 (6)	3.46 (8)	3.43 (8)
OBo	x	0.8212 (4)	0.8210 (4)	0.8217 (5)	0.8221 (5)	0.8226 (5)	0.8235 (7)	0.8238 (7)
	y	0.1084 (2)	0.1136 (2)	0.1185 (3)	0.1225 (3)	0.1282 (3)	0.1336 (5)	0.1345 (4)
	z	0.1990 (4)	0.2021 (5)	0.2071 (6)	0.2114 (6)	0.2169 (6)	0.2240 (10)	0.2242 (9)
	B	1.65 (4)	2.48 (5)	3.38 (6)	3.86 (7)	4.52 (8)	5.35 (13)	5.31 (12)
OBm	x	0.8184 (4)	0.8198 (4)	0.8208 (5)	0.8216 (5)	0.8222 (5)	0.8233 (7)	0.8239 (7)
	y	0.8470 (2)	0.8491 (3)	0.8522 (3)	0.8548 (3)	0.8593 (3)	0.8651 (5)	0.8654 (4)
	z	0.2455 (4)	0.2434 (5)	0.2402 (6)	0.2370 (6)	0.2323 (6)	0.2557 (10)	0.2252 (9)
	B	1.89 (4)	2.90 (6)	3.61 (7)	4.24 (8)	4.75 (8)	5.26 (13)	5.35 (12)
OCo	x	0.0162 (3)	0.0189 (4)	0.0210 (4)	0.0226 (5)	0.0239 (4)	0.0263 (7)	0.0266 (6)
	y	0.2902 (2)	0.2933 (2)	0.2955 (2)	0.2974 (2)	0.3005 (2)	0.3039 (4)	0.3041 (4)
	z	0.2770 (4)	0.2748 (5)	0.2709 (5)	0.2670 (6)	0.2619 (6)	0.2536 (9)	0.2534 (8)
	B	1.45 (4)	2.26 (5)	2.85 (5)	3.26 (6)	3.79 (6)	4.62 (11)	4.61 (10)
OCm	x	0.0213 (3)	0.0224 (4)	0.0236 (4)	0.0242 (5)	0.0247 (5)	0.0261 (7)	0.0264 (6)
	y	0.6873 (2)	0.6890 (2)	0.6899 (2)	0.6915 (3)	0.6933 (3)	0.6958 (4)	0.6957 (4)
	z	0.2180 (4)	0.2241 (5)	0.2310 (5)	0.2376 (5)	0.2455 (6)	0.2521 (9)	0.2525 (8)
	B	1.49 (4)	2.27 (5)	2.93 (6)	3.38 (6)	3.89 (6)	4.67 (11)	4.60 (10)
ODo	x	0.1959 (3)	0.1942 (4)	0.1927 (4)	0.1912 (5)	0.1894 (5)	0.1879 (7)	0.1882 (6)
	y	0.1123 (2)	0.1141 (2)	0.1158 (2)	0.1175 (3)	0.1198 (3)	0.1233 (4)	0.1236 (4)
	z	0.3876 (4)	0.3900 (4)	0.3928 (5)	0.3951 (5)	0.4001 (5)	0.4042 (7)	0.4050 (7)
	B	1.44 (4)	2.27 (5)	3.03 (6)	3.51 (6)	4.07 (7)	4.45 (10)	4.52 (10)
ODm	x	0.1885 (3)	0.1882 (4)	0.1881 (5)	0.1882 (5)	0.1881 (5)	0.1879 (7)	0.1875 (6)
	y	0.8675 (2)	0.8688 (2)	0.8697 (3)	0.8714 (3)	0.8736 (3)	0.8758 (4)	0.8761 (4)
	z	0.4266 (4)	0.4234 (5)	0.4195 (5)	0.4166 (5)	0.4117 (5)	0.4061 (7)	0.4056 (7)
	B	1.62 (4)	2.50 (5)	3.32 (6)	3.70 (7)	4.13 (7)	4.49 (11)	4.49 (10)
Na1*	x	0.2650 (12)	0.2702 (13)	0.2691 (14)	0.2716 (14)	0.2713 (14)	0.2709 (23)	0.2717 (20)
	y	0.9961 (8)	1.0009 (10)	1.0016 (11)	1.0026 (11)	1.0019 (12)	1.0015 (19)	1.0010 (17)
	z	0.1475 (15)	0.1620 (17)	0.1655 (18)	0.1719 (19)	0.1720 (18)	0.1723 (29)	0.1729 (27)
	B	1.54 (15)	2.45 (18)	3.19 (18)	3.76 (19)	4.18 (19)	4.86 (31)	4.84 (29)
Na2	x	0.2798 (10)	0.2800 (13)	0.2842 (14)	0.2833 (16)	0.2860 (18)	0.2896 (31)	0.2883 (29)
	y	0.9716 (6)	0.9667 (8)	0.9658 (9)	0.9626 (10)	0.9604 (12)	0.9577 (19)	0.9574 (18)
	z	0.1863 (12)	0.1767 (16)	0.1744 (18)	0.1666 (21)	0.1603 (25)	0.1537 (42)	0.1517 (40)
	B	2.19 (15)	3.44 (20)	3.98 (21)	5.00 (24)	6.53 (31)	7.75 (55)	8.14 (53)
Na3	x	0.2825 (10)	0.2849 (13)	0.2857 (16)	0.2886 (18)	0.2884 (18)	0.2895 (32)	0.2921 (29)
	y	0.0364 (6)	0.0386 (8)	0.0394 (10)	0.0415 (11)	0.0414 (11)	0.0423 (20)	0.0423 (18)
	z	0.0902 (12)	0.1032 (16)	0.1131 (22)	0.1145 (25)	0.1282 (25)	0.1392 (45)	0.1428 (41)
	B	1.79 (15)	2.76 (19)	4.40 (25)	5.46 (30)	6.02 (28)	7.84 (59)	7.84 (54)
Na4	x	0.2727 (12)	0.2683 (15)	0.2706 (16)	0.2699 (16)	0.2720 (16)	0.2754 (25)	0.2753 (22)
	y	0.0182 (8)	0.0106 (10)	0.0072 (11)	0.0052 (12)	0.0013 (13)	-0.0013 (20)	-0.0011 (18)
	z	0.1185 (15)	0.1040 (19)	0.0947 (20)	0.0942 (21)	0.0849 (21)	0.0826 (31)	0.0834 (29)
	B	1.37 (16)	2.77 (21)	3.69 (22)	4.22 (22)	5.21 (24)	5.79 (36)	5.78 (34)

* *The coordinates for the tetrahedral and oxygen atoms are those from the refinement of the single anisotropic Na atom. The coordinates for Na1, Na2, Na3, and Na4 are from a separate series of refinement cycles.*

TABLE 5. *T*-O, O-O, and Na-O interatomic distances in high albite

	24°C	350°C	600°C	750°C	950°C	1090°C	1105°C
T1o-OA1	1.646 (3)	1.644 (3)	1.643 (3)	1.650 (3)	1.648 (3)	1.649 (5)	1.649 (5)
OBo	1.648 (3)	1.644 (3)	1.640 (3)	1.641 (3)	1.636 (3)	1.640 (5)	1.632 (5)
OCo	1.638 (3)	1.647 (3)	1.646 (3)	1.642 (3)	1.645 (3)	1.642 (5)	1.643 (5)
ODo	1.653 (3)	1.653 (3)	1.654 (3)	1.651 (3)	1.650 (3)	1.644 (5)	1.646 (5)
mean	1.646	1.647	1.646	1.646	1.645	1.644	1.643
T1m-OA1	1.654 (3)	1.659 (3)	1.652 (3)	1.648 (3)	1.651 (3)	1.643 (5)	1.645 (5)
OBm	1.630 (3)	1.627 (3)	1.630 (3)	1.629 (3)	1.633 (3)	1.637 (5)	1.633 (5)
OCm	1.644 (3)	1.638 (3)	1.642 (3)	1.640 (3)	1.642 (3)	1.641 (5)	1.641 (5)
ODm	1.636 (3)	1.639 (3)	1.638 (3)	1.641 (3)	1.644 (3)	1.645 (5)	1.644 (5)
mean	1.641	1.641	1.641	1.640	1.643	1.642	1.641
T2o-OA2	1.653 (3)	1.652 (3)	1.652 (3)	1.652 (3)	1.654 (3)	1.648 (4)	1.646 (4)
OBo	1.644 (3)	1.641 (3)	1.638 (3)	1.634 (4)	1.632 (3)	1.629 (5)	1.631 (5)
OCm	1.637 (3)	1.640 (3)	1.634 (3)	1.635 (3)	1.635 (3)	1.634 (5)	1.632 (5)
ODm	1.631 (3)	1.628 (3)	1.630 (3)	1.627 (3)	1.629 (3)	1.629 (5)	1.632 (5)
mean	1.641	1.640	1.639	1.637	1.638	1.635	1.635
T2m-OA2	1.652 (3)	1.655 (3)	1.653 (3)	1.648 (3)	1.648 (3)	1.647 (4)	1.648 (4)
OBm	1.625 (3)	1.622 (3)	1.621 (3)	1.623 (3)	1.620 (3)	1.626 (5)	1.629 (5)
OCo	1.642 (3)	1.634 (3)	1.635 (3)	1.634 (3)	1.634 (3)	1.631 (5)	1.631 (5)
ODo	1.650 (3)	1.647 (3)	1.643 (3)	1.642 (3)	1.634 (3)	1.635 (5)	1.631 (5)
mean	1.642	1.640	1.638	1.637	1.634	1.635	1.635
T1o							
OA-OB	2.608 (3)	2.600 (4)	2.604 (4)	2.610 (5)	2.603 (5)	2.604 (7)	2.603 (7)
OA-OC	2.764 (4)	2.768 (4)	2.762 (4)	2.761 (5)	2.760 (5)	2.752 (7)	2.750 (7)
OA-OD	2.617 (4)	2.616 (4)	2.620 (4)	2.622 (5)	2.626 (5)	2.626 (7)	2.625 (6)
OB-OC	2.707 (4)	2.714 (4)	2.710 (4)	2.711 (5)	2.708 (5)	2.724 (8)	2.718 (7)
OB-OD	2.734 (4)	2.736 (4)	2.731 (5)	2.727 (5)	2.720 (5)	2.712 (8)	2.713 (7)
OC-OD	2.689 (3)	2.692 (4)	2.691 (4)	2.685 (5)	2.688 (5)	2.677 (7)	2.676 (7)
mean	2.687	2.688	2.686	2.686	2.684	2.683	2.681
T1m							
OA-OB	2.631 (4)	2.633 (4)	2.623 (5)	2.614 (5)	2.616 (5)	2.607 (7)	2.599 (7)
OA-OC	2.734 (4)	2.736 (4)	2.741 (4)	2.746 (5)	2.756 (5)	2.743 (7)	2.746 (7)
OA-OD	2.628 (4)	2.632 (4)	2.628 (4)	2.625 (5)	2.625 (5)	2.620 (7)	2.621 (6)
OB-OC	2.696 (4)	2.688 (4)	2.697 (5)	2.692 (5)	2.701 (5)	2.719 (7)	2.719 (7)
OB-OD	2.706 (4)	2.707 (4)	2.708 (5)	2.711 (5)	2.714 (5)	2.714 (8)	2.707 (7)
OC-OD	2.680 (4)	2.675 (4)	2.671 (5)	2.670 (5)	2.674 (5)	2.672 (7)	2.674 (7)
mean	2.679	2.679	2.678	2.676	2.681	2.679	2.678
T2o							
OA-OB	2.671 (3)	2.674 (4)	2.675 (4)	2.672 (5)	2.676 (5)	2.667 (7)	2.670 (6)
OA-OC	2.615 (3)	2.615 (4)	2.610 (4)	2.615 (4)	2.611 (4)	2.610 (7)	2.608 (6)
OA-OD	2.664 (3)	2.658 (4)	2.662 (4)	2.655 (4)	2.657 (4)	2.657 (7)	2.655 (6)
OB-OC	2.707 (4)	2.697 (4)	2.690 (5)	2.690 (5)	2.689 (5)	2.680 (8)	2.678 (7)
OB-OD	2.696 (4)	2.698 (4)	2.696 (5)	2.691 (5)	2.694 (5)	2.689 (8)	2.691 (7)
OC-OD	2.717 (3)	2.719 (4)	2.712 (4)	2.707 (5)	2.708 (5)	2.711 (7)	2.713 (7)
mean	2.678	2.677	2.674	2.672	2.673	2.669	2.669
T2m							
OA-OB	2.694 (4)	2.694 (4)	2.685 (4)	2.679 (5)	2.671 (5)	2.665 (7)	2.667 (6)
OA-OC	2.649 (3)	2.635 (4)	2.628 (4)	2.622 (4)	2.613 (4)	2.608 (7)	2.608 (6)
OA-OD	2.672 (3)	2.673 (4)	2.668 (4)	2.663 (4)	2.658 (4)	2.658 (7)	2.655 (6)
OB-OC	2.674 (4)	2.669 (4)	2.670 (5)	2.669 (5)	2.673 (5)	2.673 (8)	2.677 (7)
OB-OD	2.682 (4)	2.680 (4)	2.682 (5)	2.685 (5)	2.677 (5)	2.691 (8)	2.692 (7)
OC-OD	2.718 (3)	2.710 (4)	2.710 (4)	2.713 (5)	2.711 (5)	2.714 (7)	2.709 (7)
mean	2.682	2.677	2.675	2.672	2.667	2.668	2.668
Na-OA (1000)	2.606 (4)	2.636 (5)	2.676 (5)	2.693 (6)	2.715 (6)	2.752 (9)	2.751 (8)
OA (100C)	2.704 (4)	2.714 (5)	2.727 (5)	2.728 (6)	2.739 (6)	2.744 (9)	2.752 (8)
OA (200C)							
OA (2000)	2.340 (3)	2.363 (4)	2.382 (4)	2.402 (5)	2.414 (5)	2.436 (7)	2.439 (6)
OA (200C)							
OB (000C)	2.512 (4)	2.583 (4)	2.661 (5)	2.723 (6)	2.810 (6)	2.907 (10)	2.918 (9)
OB (m00C)	3.186 (5)	3.168 (6)	3.144 (7)	3.100 (7)	3.025 (7)	2.932 (10)	2.927 (9)
OC (0210)	3.371 (4)	3.326 (5)	3.275 (6)	3.245 (6)	3.197 (6)	3.136 (9)	3.134 (8)
OC (m210)	2.917 (4)	2.958 (5)	3.000 (6)	3.031 (6)	3.068 (6)	3.132 (9)	3.130 (8)
OD (0000)	2.497 (3)	2.545 (4)	2.600 (5)	2.653 (6)	2.737 (6)	2.830 (9)	2.835 (9)
OD (m000)	3.133 (5)	3.085 (6)	3.024 (7)	2.985 (7)	2.928 (7)	2.851 (10)	2.846 (9)
mean	2.807	2.820	2.832	2.840	2.848	2.857	2.859

parameters approaching the transition to monalbite was checked independently for different crystals by different people, and although there is some uncertainty in our temperature measurement, it is certain that the transition temperature is significantly higher than those found by other investigators.

When the single crystals of high albite were quenched from the temperature range where they approached monoclinic symmetry, the crystals were always found to have albite twinning, despite our observation that the crystals were still single before quenching. On *hk*0 precession photographs of quenched crystals, diffuse streaks extend from the spots in the room-temperature pattern toward the positions of the spots at high temperature. These diffuse streaks are larger for the reflections which have larger *h* components in their *hkl* indices and smaller for the reflections which have larger *k* components. These diffuse streaks suggest that some parts of the crystal did not completely recover their unit cells in the cooling procedure, but were closer to monoclinic symmetry than the other parts of the crystal. All parts of the crystal maintain the same *b* direction at any temperature.

It has been generally observed for many materials that on cooling from temperatures above a transition point, the crystal becomes an aggregate of fine twinning because of the effect of changing the symmetry from higher to lower at the transition temperature. In the case of albite, this phenomenon was observed in spite of the observation that the crystal did not attain truly higher symmetry, even though it approached very closely to it. This may be explained if we accept the multipartite unit-cells and fault domain structure proposed for high albite by Ribbe *et al.* (1969). If, in this hypothetical structure, some of the domains have actually been transformed to the monoclinic structure at high temperature even though other parts are still triclinic, these monoclinic parts can induce albite twinning on cooling. Pericline twinning was also observed after quenching, but the relative amount was always very small compared with that of albite twinning. It is impossible to distinguish whether monalbite is truly monoclinic or whether it is composed of triclinic cells with $\alpha = \gamma = 90°$. The observation that α^* and γ^* appear to remain at 90° at temperatures higher than the transition plus the trend toward equivalence of intensities, *i.e.*, $I(hkl) \equiv I(h\bar{k}l)$, as a function of temperature supports a monoclinic symmetry.

Results

Crystal structures

The crystal structures of low albite and high albite have been described in detail by Ribbe *et al.* (1969) and by Smith (1974). Therefore, we will not attempt to repeat the detailed descriptions except where necessary to contrast the structural behavior at high temperature. Figure 1 is a projection along a^* of a monoclinic feldspar structure; this diagram may be used as a reference to the atom labels in the discussions that follow. Note that in low albite the *T*1*o*

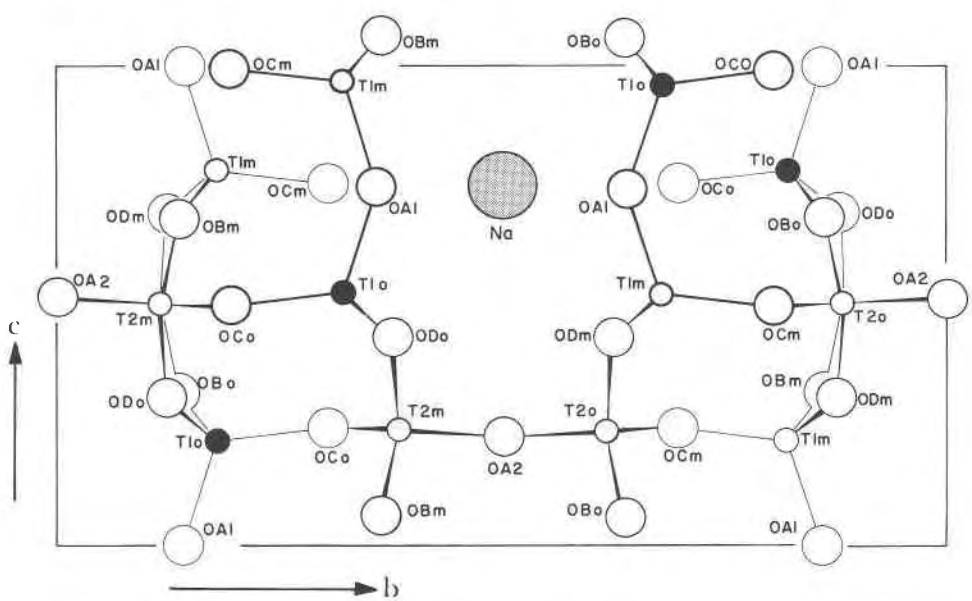

FIG. 1. Projection along a^* of a monoclinic feldspar structure.

site is the site which is fully occupied with Al. As disorder increases, Al becomes distributed throughout the other three sites, in approximate proportion to the amount of disorder until, in maximum high albite, the disorder is complete.

Interatomic distances

Table 5 shows how the *T*–O distances vary with temperature. As with many other silicate structures the average (Si,Al)–O distances remain nearly constant as the temperature is increased. Because the temperature factors increase significantly with temperature, it is obvious that thermal corrections would result in an apparent expansion of the Si,Al–O bonds; however, it is not clear what thermal model should be used or how the results of a thermal correction could be used to advantage for this paper. We are more interested in relative trends of interatomic distance with temperature rather than in absolute values. For example, the average distance in *T*1*o* at room temperature is slightly larger (~ 0.005Å) than in the other tetrahedra, indicating perhaps that it contains more Al than the others. However, at 1105°C *T*1*o* and *T*1*m* are almost equal (1.643Å and 1.641Å) as are *T*2*o* and *T*2*m* (1.635Å). It is a requirement of the *C*2/*m* symmetry of monalbite that *T*1*o* ≡ *T*1*m* and *T*2*o* ≡ *T*2*m*, but *T*1 does not have to be equivalent to *T*2.

The magnitudes of the changes in individual *T*–O distances are correlated with the changes in Na–O distances. For example, in Figure 2 the distances from Na to O*Bm*, *ODm*, and to O*Bo*, O*Do* change rapidly because each O*B* pair and each O*D* pair must become equivalent at the transition to monalbite. From Table 5 it can be seen that the *T*–O*Bm* and *T*–O*Dm* distances increase and the *T*–O*Bo* and *T*–O*Do* distances decrease with temperature. Similar correlations can be made for other sets of interatomic distances.

In the room-temperature structure of high albite, there are six Na–O bonds within 3.0Å. All of these bonds expand with increasing temperature, but Na–O*A*2 is the shortest bond length at all temperatures. The other bonds change their relative sequence in length (Fig. 2) at high temperature with Na to O*Cm* increasing beyond 3.0Å and to O*Bm* and O*Dm* decreasing below 3.0Å. If this somewhat arbitrary limit is selected for determining coordination number, then the coordination of Na increases from six to seven at about 600°C.

Temperature factors

Variations of equivalent isotropic temperature factors for Na (single- and quarter-atom models), *T* (mean values) and O (mean values) atoms are plotted as functions of temperature with extrapolation to 0° K in Figure 3. This kind of plot was used by Quareni and Taylor (1971) in their study of low albite at high temperature as evidence for determining whether the observed thermal parameters were due to true thermal motion or spatial disorder. Their assumption was that if thermal motion was the sole cause of the observed values for *B*, the isotropic *B*'s should extrapolate to zero at 0°K. In their experiments, the Na and tetrahedral *B*'s did extrapolate approximately to zero whereas those for oxygen did not. Figure 3 shows that our results for *T* and O atoms in high albite are similar to those of Quareni and Taylor (1971) for low albite, but the *B*'s indicate some spatial disorder for both kinds of atoms.

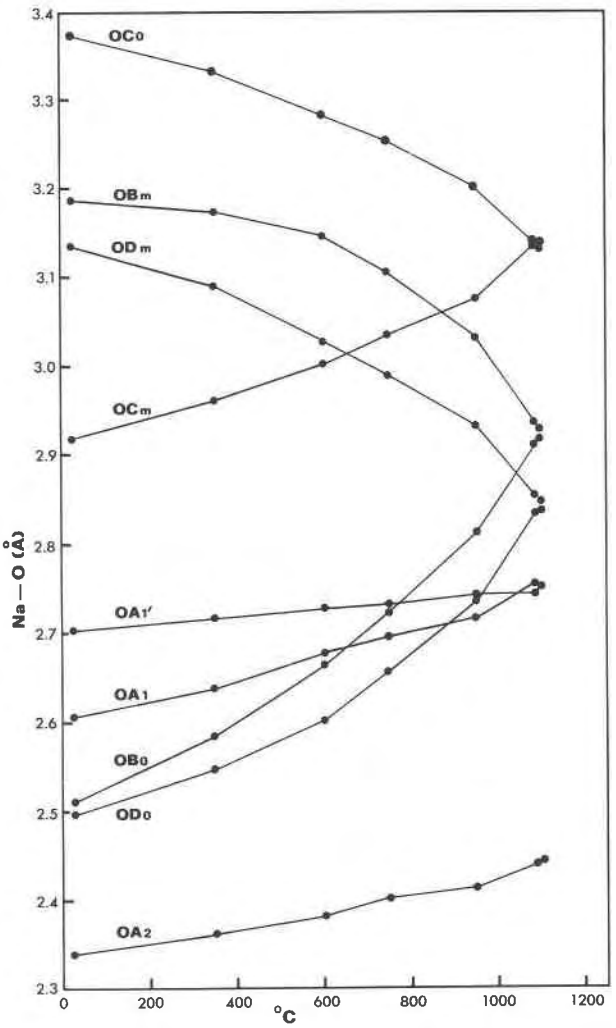

FIG. 2. Na–O distances *vs.* temperature in high albite.

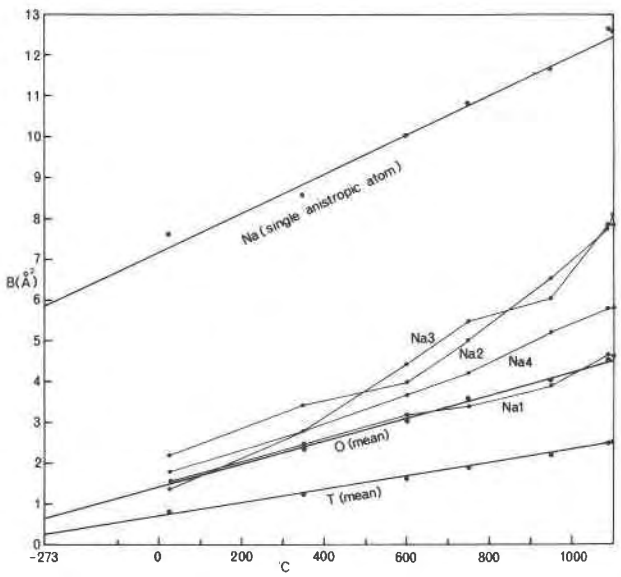

FIG. 3. Equivalent isotropic temperature factor *vs.* temperature for a single anistropic Na atom, four quarter atoms (Na1, Na2, Na3, and Na4), tetrahedral, and oxygen atoms.

Table 4 shows that the temperature factors for each of the *T* atoms are almost identical to one another throughout the temperature range. O*A*2, the oxygen atom closest to Na, and consequently, the most tightly bound oxygen atom in the structure, has the smallest temperature factor. Presumably because they are less tightly bound to Na, the "*m*" oxygen atoms have larger *B*'s than do the "*o*" oxygen atoms. However, as expected, the *B*'s for each "*m*" and "*o*" pair converge to a common value at the transition to monalbite.

Discussion

Maximum high albite

Mackenzie (1952) studied a series of natural and synthetic albites at high temperature, using a powder diffractometer to measure the separation of the 111 and $1\bar{1}1$ peaks as a function of temperature. He found that at temperatures around 1000°C, the two peaks (as well as other similarly related peaks) merged into a single peak that remained single under further heating. This was taken as evidence of a transition to a monoclinic (or pseudomonoclinic) symmetry. He also found that the temperature of the transition was a function of the synthesis conditions and/or prior heat treatment of the sample, and that it decreased with orthoclase content and increased with anorthite content.

In a subsequent paper, Mackenzie (1957) reported additional experiments and concluded that a continuous series, primarily a function of Al/Si order, exists between low albite and high albite. Only the most disordered crystals (those crystallized above 950°C) were observed to undergo a change to monoclinic symmetry at high temperature. Grundy *et al.* (1967) examined a natural albite crystal ($Ab_{99.26}$) which had been heated for thirty-one days at 1060°C. Using a precession camera equipped with a furnace, they determined a transition to monalbite at 930°C. In more extensive experiments with both powders and single crystals, Grundy and Brown (1969) detected transitions in several different samples with different pressure–temperature histories. Using twinned Amelia albite crystals which had been annealed at above 1080°C for 3200 hours, Okamura and Ghose (1975) reported a transition at 930°C.

Cell parameters

Figure 4 is a display of the α^*–γ^* angles obtained from our high-temperature experiments plus those of

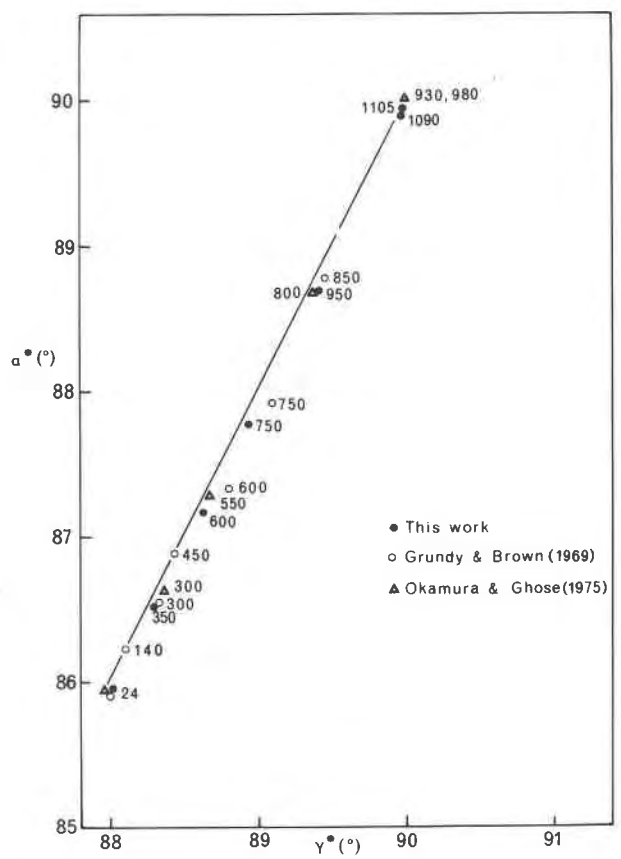

FIG. 4. Variation of α^* and γ^* as functions of temperature for three different high albite crystals.

Grundy and Brown (1969) for their sample #307 and those of Okamura and Ghose (1975). The straight line in Figure 4 joins the point representing the α^*–γ^* values for analbite given by Stewart and Wright (1974) to the point for a monoclinic feldspar where $\alpha^* = \gamma^* = 90°$. Any significant departure to the right of this line indicates Al/Si ordering (towards low albite). The α^* *vs.* γ^* variations for these three samples are remarkably similar, except for the temperatures at which equivalent α^*–γ^* values are reached. Apparently additional criteria are needed to specify the structural state of high albite at any given temperature.

Sodium atom

One of the purposes of this research was to see whether further insight could be gained about the nature of the Na position in high albite. For low albite, Ribbe *et al.* (1969) discussed the evidence for anisotropic thermal vibration *vs.* a space averaging over two possible positions for Na. Their conclusion, which also took into account the two-dimensional study of low albite by Williams and Megaw (1964) at −180°C, was that "it is not possible, on the structural evidence available, to decide whether the anisotropy of the sodium atom represents anisotropic thermal vibration or a space average; with due caution it is permissible to say only that the low-temperature measurements have their most obvious explanation in terms of space average." However, Quareni and Taylor (1971) found that the apparent ansiotropy of thermal vibration increases as a function of temperature and felt that this was sufficient evidence to support true anisotropic thermal vibration as an explanation for the Na anisotropy in low albite.

For high albite, Ribbe *et al.* (1969) found that the quarter-atom model clearly gave the best agreement with their data. These authors discussed the possible existence of "multipartite cells and fault domains" as explanations for the high albite structure. Our room-temperature results confirm that using four isotropic Na atoms, each included in the least-squares refinement with an occupancy factor of ¼, gives better agreement between observed and calculated structure factors than does a single anisotropic Na atom. However, there is no significant difference in R for the two models at high temperatures. In the refinement of the 24°C data, the starting coordinates for the quarter-atoms were those of Ribbe *et al.* (1969). Our final refined coordinates were similar to the original ones with the four sites in a row as shown in Figure 5*a*. Here the outer pair and inner pair are

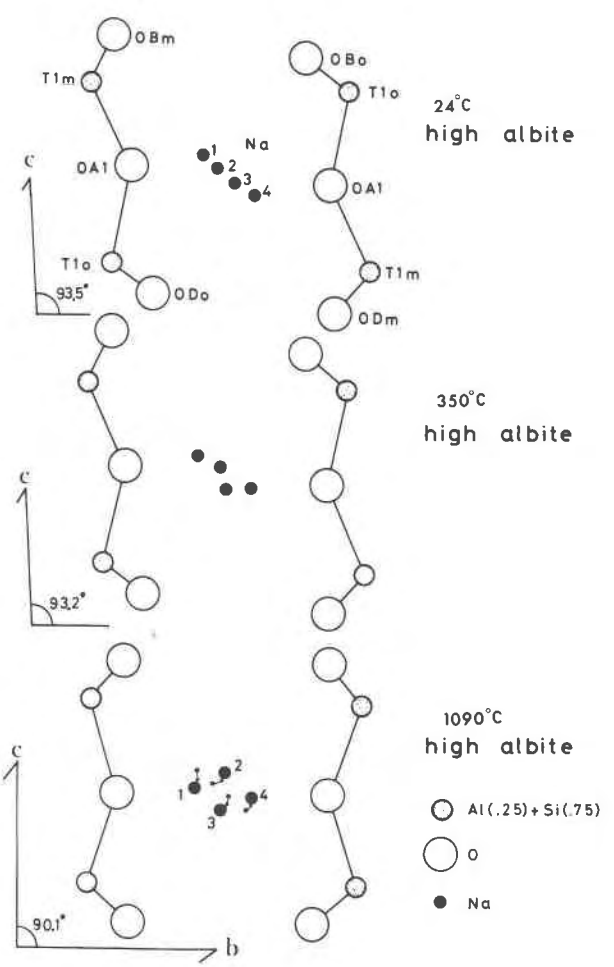

FIG. 5. Refined positions of Na quarter-atoms at three temperatures, (a) 24°C, (b) 350°C, and (c) 1090°C.

separated by 1.12Å and 0.38Å, respectively. This linear orientation is parallel with the major axis of the anisotropic thermal ellipsoid in the single-atom model. For each refinement using high-temperature data, the starting coordinates were the final coordinates of the next lower temperature. Figures 5b and 5c show what happens to the quarter atoms as the temperature is raised. At 1090°C, the structure is nearly monoclinic with Na2 and Na3 moving onto the mirror plane and Na1 and Na4 becoming a mirror-related pair. This arrangement can apparently be described equally well by either model and thus there is no difference in R between the models.

Whether there is physical significance in the quarter-atom model cannot be proved by these results, although the plots of B *vs.* temperature in Figure 3 support the idea that it is certainly better than the single-atom model. In Figure 3 the temperature fac-

tor for the single Na atom extrapolates to approximately 6Å^2 at −273°C, whereas the B's for each of the quarter atoms extrapolate to values around 1Å^2. An interpretation of this might be that there are four possible kinds of domains, each of which contains Al in one of the four T sites, but with the Al-avoidance rules holding for each domain. The specific Al/Si arrangement in a domain determines the Na position. Superimposed on this is the large anisotropic thermal motion observed for Na in low albite (Quareni and Taylor, 1971).

Whether high or low albite contains domains is open to question. No satellite reflections have been observed in pure albite although McLaren (1974) observed a lamellar structure with the electron microscope in $Ab_{98}An_2$ with 250Å periodicity; the latter is probably a result of a peristeritic kind of exsolution. In diffraction patterns of this material, no superstructure reflections were observed; the lamellar structure caused continuous radiation streaks to be associated with the class *a* reflections. Recently, Kitamura and Morimoto (1975) have proposed a structure for intermediate plagioclase which is based on two modulation waves of different wavelength, a density wave resulting from varying composition and a displacement wave resulting from the displacement of Na and Ca from mean positions. Kitamura and Morimoto show that the displacement vectors for intermediate plagioclase are in approximately the same direction as they would be in low albite; hence, it is likely that a similar model could be applied to high albite. This application is, however, outside the scope of the present paper.

Monalbite

One of the purposes of this investigation was to determine the crystal structure of monalbite, which has been reported to form when the most disordered high albite is heated to about 980°C. A number of determinations of the transition temperature have been made, varying from 930°C to about 1100°C (Smith, 1974, p. 292–305). However, it is now apparent that some of the investigators reported transition temperatures on intermediate albites or on ones containing small amounts of potassium or calcium. The question of the structural state of the albite used in our experiments is a serious one, and we can only report what we have observed—the fact is that our high-albite crystal never did become absolutely monoclinic within the range of the experiments.

Grundy and Brown (1969) carried out an extensive series of experiments on albites of varying structural states. In these experiments, they used a precession camera with a heating attachment to measure cell parameters as a function of temperature. Their conclusion which agrees with other investigators (Laves, 1960; Kroll and Bambauer, 1971; Okamura and Ghose, 1975; Duba and Piwinskii, 1974) is that the transition temperature of pure albite in the most disordered form is in the range of 930–980°C. Our experiments, which did not confirm a transition as high as 1105°C, may have used a crystal that was not completely disordered. Alternatively, it is possible that the sensitivity of our measurements on the single-crystal diffractometer was greater than can be obtained with the precession camera or powder diffractometer as used by others. Nevertheless, at the highest temperatures our albite was so close to being topologically monoclinic that the atom parameters and the derived interatomic distances and angles given here are essentially those of monalbite.

The statement by Grundy *et al.* (1967) that it is not possible to define high albite on the basis of its lattice parameters at room temperature alone is supported by the present investigation. Table 6 lists several sets of cell parameters published for high albite plus $\Delta 2\theta(2\theta_{131}-2\theta_{1\bar{3}1})$ often used to indicate the structural state of albite. It is generally accepted that the larger the $\Delta 2\theta$ value, the more disordered the albite. Our crystal and that of Okamura and Ghose (1975) have almost identical cell angles and $\Delta 2\theta$ (the cell edge differences are probably due to the limitations of using precession photographs to determine cell edges), yet the apparent transition temperatures differ by almost 100°C. Figure 6 is a plot of α^* and γ^* *vs.* temperature for our and Okamura and Ghose's crystals. The angles are identical at 24°C, but diverge as the temperature is increased. The other cell parameters behave similarly. One obvious interpretation of Figure 6 is that one or both of the experimental temperature scales are in error. However, we performed the experiment on several different crystals with a carefully calibrated crystal heater and obtained comparable results each time. Nevertheless, this problem cannot be resolved completely until identical experiments are performed on different crystal samples.

If cell parameters are not reliable guides to maximum high albite, what are the differences in the crystals? Our single crystals were synthesized hydrothermally and annealed at 1060°C for forty days. Okamura and Ghose's were twinned Amelia albite which had been annealed above 1080°C for 3200 hours (133 days). Okamura and Ghose did not pub-

TABLE 6. Cell parameters of different high albites

	a,a^*	b,b^*	c,c^*	α,α^*	β,β^*	γ,γ^*	V,V^*	$\Delta 2\theta^\dagger$
This work 24°C	8.1535	12.8694	7.1070	93.521	116.458	90.257	665.95	
	0.137083	0.077900	0.157564	85.938	63.470	87.957	0.001502	2.005
Okamura & Ghose (1975) 27°C	8.1400	12.8500	7.0900	93.520	116.550	90.250	661.73	
	0.137420	0.078018	0.158068	85.939	63.378	87.959	0.001511	2.009
Grundy & Brown (1969) #307(25°C)	8.1570	12.8880	7.1130	93.580	116.490	90.190	667.61	
	0.137046	0.077791	0.157467	85.905	63.451	88.001	0.001498	2.001
Grundy & Brown (1969) #307(25°C)	8.1550	12.8760	7.1140	93.600	116.450	90.120	667.11	
	0.137038	0.077861	0.157402	85.919	63.485	88.072	0.001499	1.976
Wainwright & Starkey, Tiburon albite	8.1520	12.8580	7.1080	93.589	116.455	90.115	665.35	
	0.137094	0.077969	0.157538	85.933	63.481	88.983	0.001503	1.970
Smith (1974) Table 7-1, p. 219	8.1600	12.8730	7.1100	93.520	116.430	90.270	667.11	
	0.136941	0.077879	0.157460	85.934	63.497	87.946	0.001499	2.009
Kroll (1971), from Smith (1974)	8.1560	12.8720	7.1110	93.480	116.440	90.240	666.81	
	0.137016	0.077879	0.157440	85.993	63.491	87.998	0.001500	1.973
Stewart & Von Limbach (1967)	8.1600	12.8700	7.1060	93.545	116.363	90.183	666.98	
	0.136854	0.077895	0.157454	85.949	63.569	88.030	0.001499	1.979

$^\dagger \Delta 2\theta = 2\theta(131) - 2\theta(\bar{1}31)$.

lish a chemical analysis of their crystal, but we have made microprobe analyses of an Amelia albite crystal as well as the annealed high albite sample used in our experiments. The results are:

Amelia albite (average of three points)—
$Or_{0.6}Ab_{99.3}An_{0.1}$

Synthetic high albite (average of nine points)—
$Or_{0.5}Ab_{98.3}An_{1.2}$

The slightly higher An content of the synthetic material could have some effect on the transition temperature, but the work of Mackenzie (1952) indicates that it would take about 10 percent An to change the inversion temperature by 90°C. The fact that the Okamura and Ghose material was heavily twinned might affect the transition temperature, although Grundy *et al.* (1967) reported a transition temperature of 980°C for an untwinned synthetic crystal which had been annealed for thirty-one days at 1060°C.

It does appear that different crystals with very similar cell dimensions but different provenance exhibit different transition temperatures. It should be pointed out, however, that all of the previous work (Mackenzie, 1952; Grundy *et al.*, 1967; Kroll and Bambauer, 1971; Okamura and Ghose, 1975) used either powder diffractometers or precession cameras to determine when monoclinic symmetry had been reached. Neither of these techniques is sensitive enough to detect small *metric* departures from monoclinic symmetry nor are they able to distinguish between twinned triclinic albite with $\alpha = \gamma = 90°$ and monalbite. It is possible that our crystal did not become monoclinic because of the small An content; it is also possible that if high albite is composed of domains, each domain remains triclinic (because of the Al/Si distribution) and the observed pseudo-monoclinic symmetry is just a result of the domains adapting themselves to one another at high temperature. Certainly, if Al-avoidance is dominant, most unit cells must still be triclinic at any temperature because of the asymmetric Al/Si distribution in the tetrahedral sites.

Conclusions

These high-temperature experiments have shown that high albite does approach a monoclinic symmetry at high temperature; however, careful measurements of cell parameters indicate that the crystals used in this study did not become exactly monoclinic at 1105°C; although, when cooled from this temperature, the resulting crystals always showed albite twinning (and, to a lesser extent, pericline twinning). From comparison with experiments performed by others, it is apparent that cell parameters alone are not sufficient to characterize the structural state of high albite. Additional criteria must include the presence or absence of twinning or other structural perturbations as well as chemical composition. The R factors and the extrapolation to 0°K of isotropic temperature factors indicate that Na is better described by the quarter-atom model than as a single anisotropic atom. At high temperatures, however, the R factors are nearly identical for the two models, but temperature-factor extrapolation supports the quar-

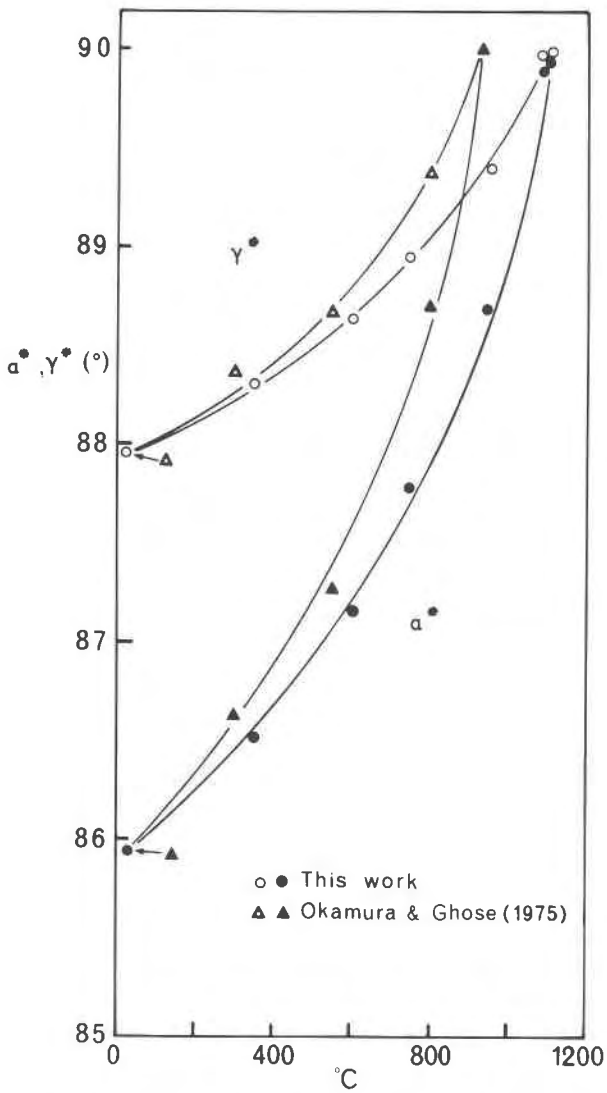

FIG. 6. Variation of α^* and γ^* as functions of temperature showing that although the values for two different crystals are identical at 24°C, they diverge at high temperature and indicate two different temperatures for the transition to monalbite. Although this difference could be a result of errors in temperature measurement, the available evidence suggests that it is caused by differences in the physical properties of the materials examined.

ter-atom model. In addition, all atoms appear to be disordered in a static fashion with Na exhibiting much more displacement than the framework atoms.

Acknowledgments

The authors would like to thank Kenneth Baldwin for his extensive help with the laboratory experiments and Shirley King for typing the manuscript. Dr. Gary Lofgren (NASA Johnson Space Center) kindly provided the intermediate albite crystals used in this study. This research was supported by the Earth Sciences Section, National Science Foundation, NSF Grant #A041137.

References

BROWN, G. E., S. SUENO AND C. T. PREWITT (1973) A new single-crystal heater for the precession camera and four-circle diffractometer. *Am. Mineral.* **58,** 698–704.

DOYLE, P. A. AND P. S. TURNER (1968) Relativistic Hartree-Fock x-ray and electron scattering factors. *Acta Crystallogr.* **A24,** 390–397.

DUBA, A. AND A. J. PIWINSKII (1974) Electrical conductivity and the monoclinic–triclinic inversion in albite. *EOS Trans. Am. Geophys. Union,* **56,** 1201.

FERGUSON, R. B., R. J. TRAILL AND W. H. TAYLOR (1958) The crystal structures of low-temperature and high-temperature albite. *Acta Crystallogr.* **11,** 331–348.

GRUNDY, H. D. AND W. L. BROWN (1969) A high-temperature x-ray study of the equilibrium forms of albite. *Mineral. Mag.* **37,** 156–172.

———, W. L. BROWN AND W. S. MACKENZIE (1967) On the existence of monoclinic $NaAlSi_3O_8$ at elevated temperatures. *Mineral. Mag.* **36,** 83–88.

HARLOW, G. E., G. E. BROWN AND W. C. HAMILTON (1973) Neutron diffraction study of low albite. *EOS Trans. Am. Geophys. Union,* **54,** 497.

KITAMURA, M. AND N. MORIMOTO (1975) The superstructure of intermediate plagioclase. *Proc. Japan Acad.* **51,** 419–424.

KROLL, H. AND H. U. BAMBAUER (1971) The displacive transformation of (K, Na, Ca) feldspars. *Neues. Jahrb. Mineral. Monatsh.* 413–416.

LAVES, F. (1960) Al/Si-Verteilungen, Phasen-Transformationen und Namen der Alkalifeldspäte. *Z. Kristallogr.* **113,** 265–296.

MACKENZIE, W. S. (1952) The effect of temperature on the symmetry of high-temperature soda-rich feldspars. *Am. J. Sci., Bowen Volume,* 319–342.

——— (1957) The crystalline modifications of $NaAlSi_3O_8$. *Am. J. Sci.* **255,** 481–516.

MCLAREN, A. C. (1974) Transmission electron microscopy of the feldspars. In, W. S. MacKenzie and J. Zussman, Eds., *The Feldspars.* Manchester University Press, 378–423.

MEGAW, H. D. (1956) Notation for feldspar structures. *Acta Crystallogr.* **9,** 56–60.

——— (1974) The architecture of the feldspars. In, W. S. MacKenzie and J. Zussmann, Eds., *The Feldspars.* Manchester University Press, 2–24.

OKAMURA, F. P. AND S. GHOSE (1975) Analbite–monalbite transition in a heat-treated twinned Amelia albite. *Contrib. Mineral. Petrol.* **50,** 211–216.

PHILLIPS, M. W. AND P. H. RIBBE (1973) The variation of tetrahedral bond lengths in sodic plagioclase feldspars. *Contrib. Mineral. Petrol.* **39,** 327–339.

PREWITT, C. T. AND A. W. SLEIGHT (1968) Structure of $Gd_{22}S_3$. *Inorg. Chem.* **7,** 1090–1093.

———, S. SUENO AND J. J. PAPIKE (1974) Models for albite in different structural states. *EOS Trans. Am. Geophys. Union.* **55,** 464.

QUARENI, S. AND W. H. TAYLOR (1971) Anisotropy of the sodium atom in low albite. *Acta Crystallogr.* **15,** 1017–1035.

RIBBE, P. H., H. D. MEGAW, W. H. TAYLOR, R. B. FERGUSON AND R. J. TRAILL (1969) The albite structures. *Acta Crystallogr.* **B25,** 1503–1518.

SMITH, J. V. (1974) *Feldspar Minerals,* Vol. 1. Springer-Verlag, Berlin, Heidelberg, New York.

STEWART, D. B. AND T. L. WRIGHT (1974) Al/Si order and symmetry of natural alkali feldspars, and the relationship of strained

cell parameters to bulk composition. *Bull. Soc. fr. Minéral. Crist.* **97,** 356–377.

SUENO, S., C. T. PREWITT AND J. J. PAPIKE (1973) High-temperature crystal chemistry of albite. *EOS Trans. Am. Geophys. Union.* **54,** 1230.

TAYLOR, W. H. (1933) The structure of sanidine and other felspars. *Z. Kristallogr.* **85,** 425–442.

WILLIAMS, P. P. AND H. D. MEGAW (1964) The crystal structures of high and low albites at −180°C. *Acta Crystallogr.* **17,** 882–890.

Manuscript received, November 28, 1975; accepted for publication July 14, 1976.